



NANYANG  
TECHNOLOGICAL  
UNIVERSITY

# LV Distribution, Performance and Applications

Presented by: Bi Guoan

School of Electrical and Electronic Engineering  
Nanyang Technological University  
Singapore

# Outline

---

## □ Introduction

## □ Lv distribution (LVD)

- Definition and properties
- Performances

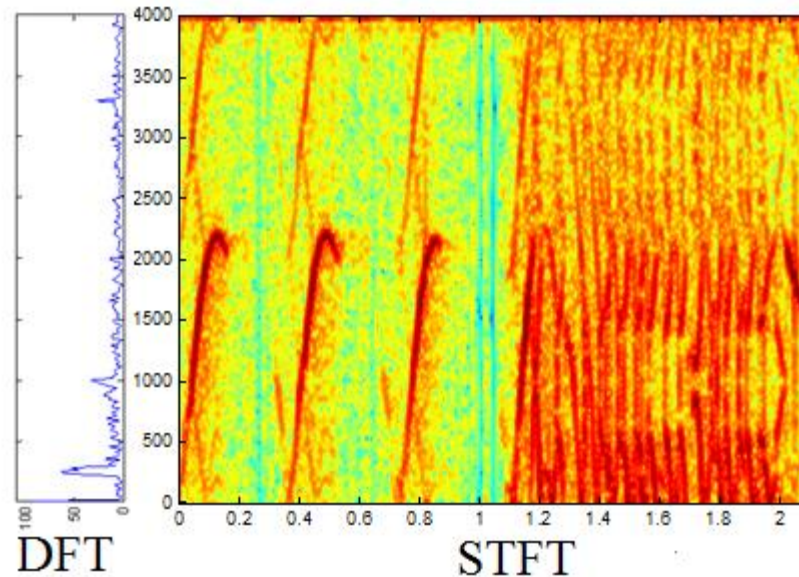
## □ Application

- SAR image processing
- CS based SAR image processing

## □ Conclusion

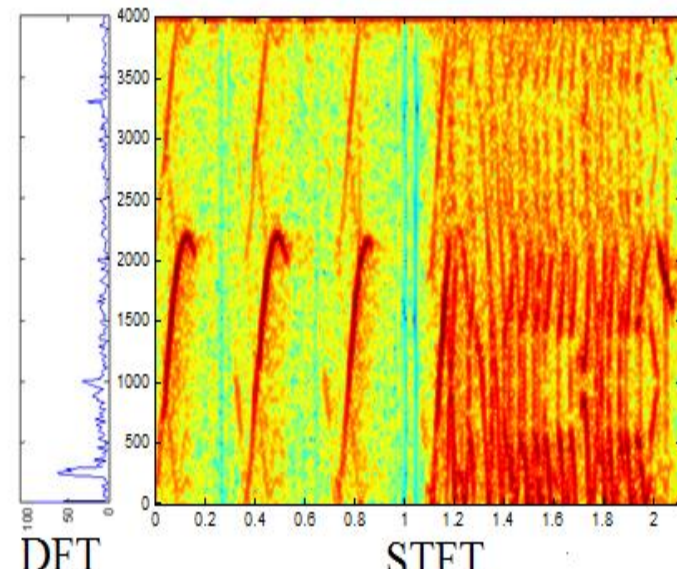
# Introduction

- Most real signals contain frequencies varying with time – known as non-stationary or time-varying
- Fourier transform tells us the frequencies in the signals, but not how they change.
- Time frequency signal analysis has been useful to truthfully reveal the useful information matching with our observations, [Example](#).



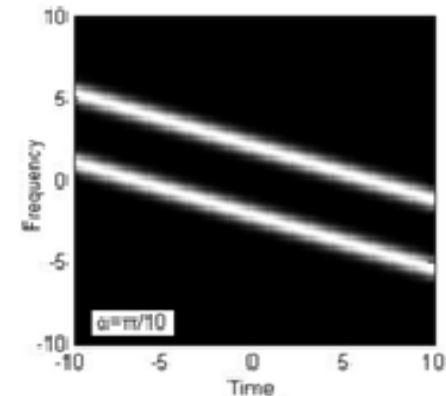
# Introduction

- A time–frequency distribution should have the following desirable features:
    - **High signal concentration** for easier analysis and interpretation.
    - **No cross-term** to avoid confusing components duo to the imperfection of the processing methods
    - Desirable **mathematical properties** ensure such methods beneficial to real-life applications.
    - **Lower computational complexity** to ensure the time needed to process the signal for real-time implementations.
    - **Others ...**



# Introduction

- Well known time frequency representations (TFRs):
  - STFT (Gabor transform):** simple with low resolution limited to uncertainty principle (TFR).
  - Local Polynomial periodogram (LPP):** requires much more computation for estimation of polynomial coefficient (TFR)  $e^{j(\omega_0 t + \omega_1 t^2 + \omega_2 t^3 \dots)}$
  - Bilinear WVD, SWVD:** providing best signal concentration, but suffering from the cross-term for multi-component signals (TFR)
  - Fractional Fourier transform:** a rotation operation on TFRs to find the best signal concentration
  - Wavelet transform:** no direct physical meaning from the results



# Introduction

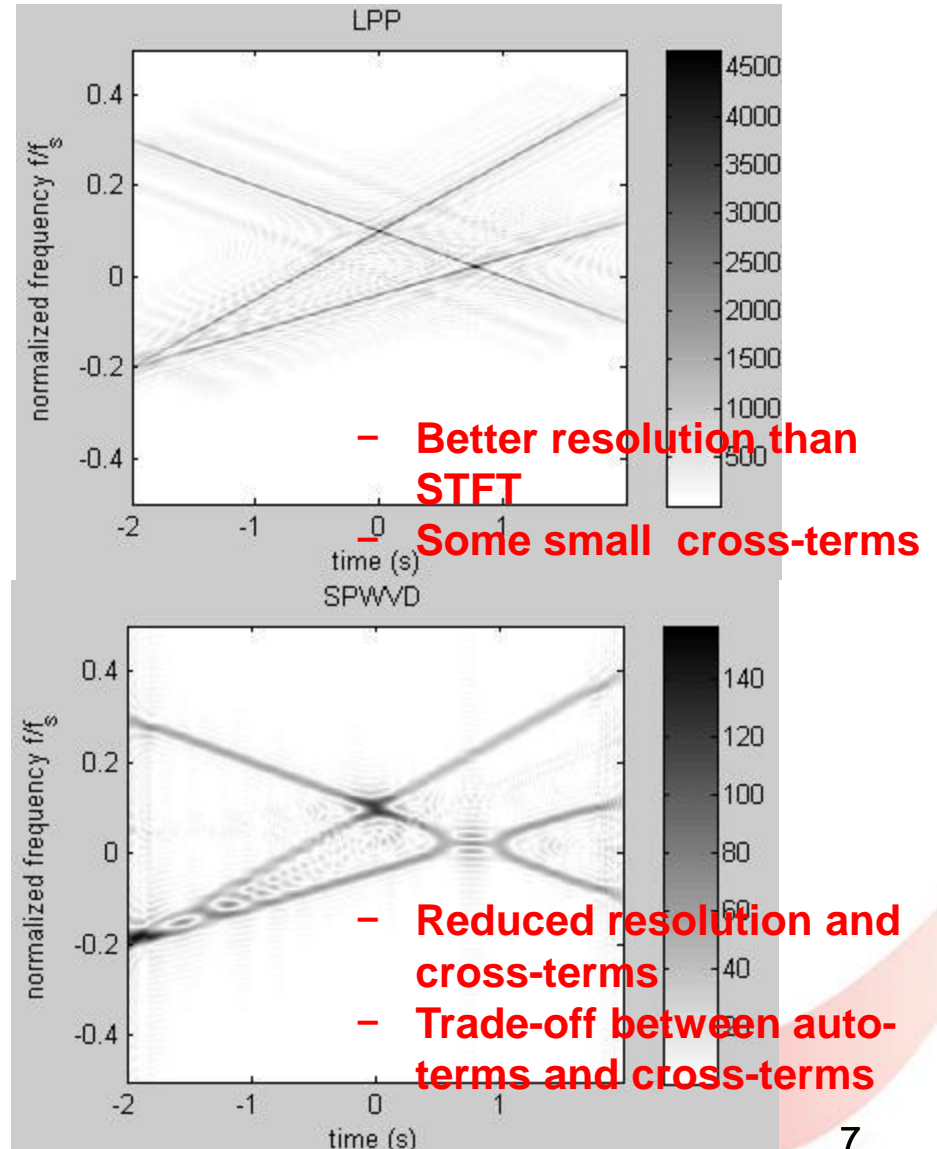
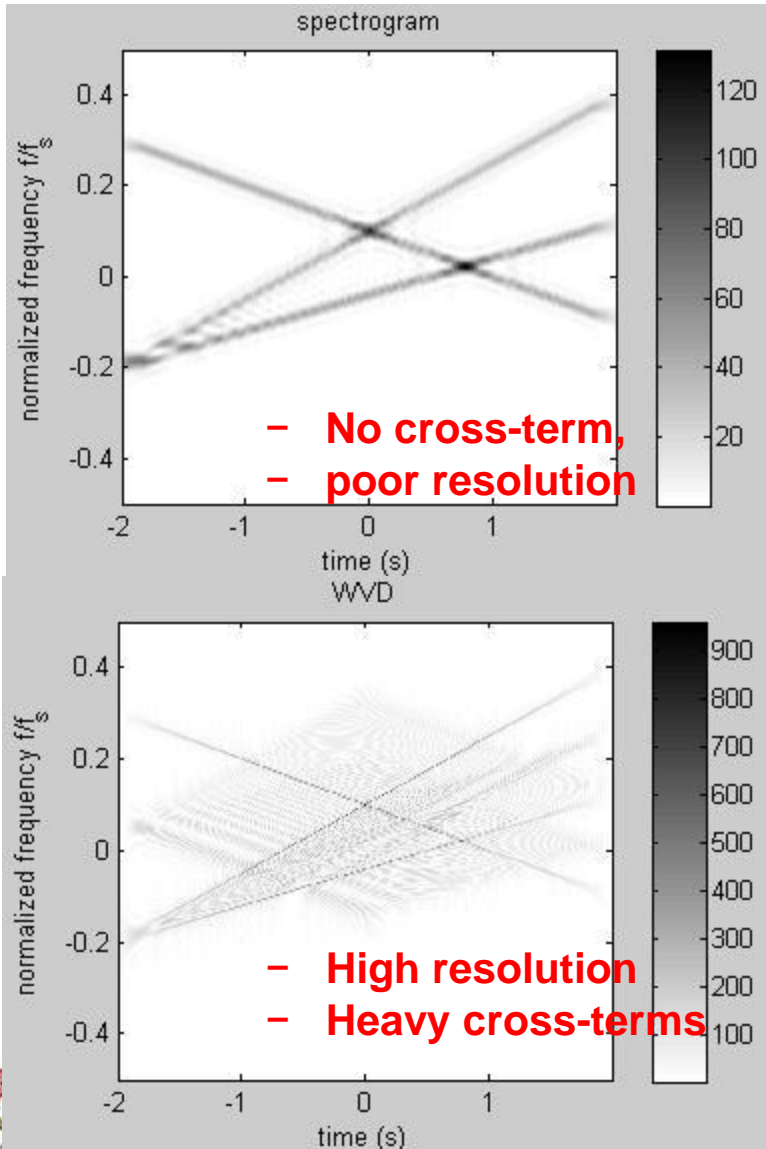
- The frequencies of time varying signals may change in various ways.
- Within a short time period, we assume the frequencies are changing linearly
  - Linear frequency modulated (LFM) signal:

$$x(t) = \sum_{k=1}^K x_k(t) = \sum_{k=1}^K A_k \exp\left(j2\pi f_k t + j\pi\gamma_k t^2\right)$$

  
centroid frequency      chirp rate

- Two types of signal representations:
  - Time-frequency representations (TFRs)
  - Frequency chirp rate representations (FCRs)

# Introduction



# Introduction

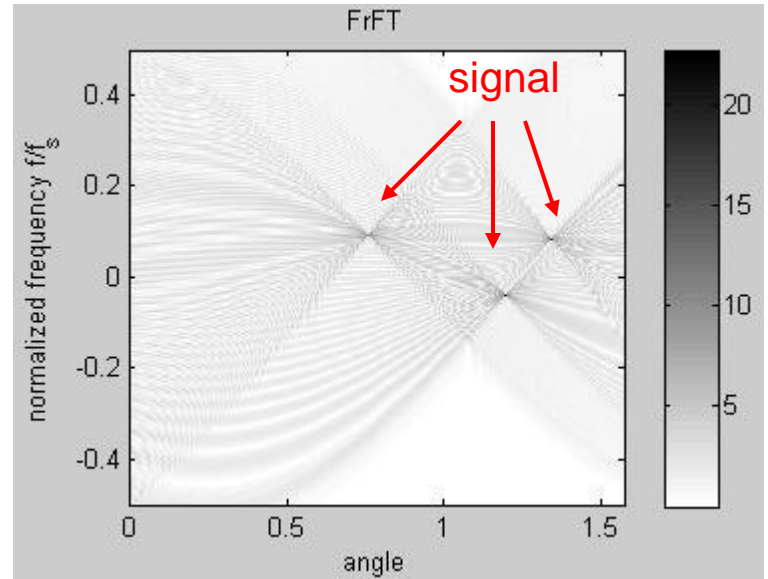
- Frequency-chirp rate representations (FCRs)
  - Directly providing signal parameters, such as frequencies and chirp rate;
  - Methods based on FT-related transform and searching, such as polynomial Fourier transform (PFT), and Fractional FT ([FrFT](#))
  - Methods based on TFRs and integration, such as LPP-Hough transform, Wigner-Hough transform (WHT) and Radon-Wigner transform, etc.

# Introduction

- Frequency-chirp rate representations (FCRs)
  - The FrFT, a widely used method:

$$K_\alpha(t, u) = \begin{cases} \delta(t-u), & \text{Searching angle} \\ \delta(t+u), & \alpha = 2n\pi \\ \sqrt{\frac{1-j \cot \alpha}{2\pi}} e^{j\frac{u^2+t^2}{2}\cot \alpha - jut \csc \alpha}, & \alpha + \pi = 2n\pi \\ , \text{ otherwise} \end{cases}$$

$$X_{FrFT}(\alpha, u) = \int_{-\infty}^{\infty} x(t) K_\alpha(t, u) dt$$



FrFT of the 3-component LFM signal

- No cross-term, reasonable resolution/concentration

# Introduction

- For critical environments, such as very low SNR and multiple signal components, most of these methods are not usable.
- Other suitable methods are required to obtain a balanced performance among a few **contradictory** requirements
  - High signal concentration with strong noise environment
  - Low cross-terms among different components
  - High signal resolution and
  - Low computation complexity
- LV distribution (LVD) is a new algorithm achieving the above requirements

# Outline

## □ Introduction

## □ Lv distribution (LVD)

- Definition and properties
- Performances

## □ Application

- SAR image processing
- CS based SAR image processing

## □ Conclusion

# Lv distribution (LVD)

- The LVD
  - Combines the desirable properties of linear and bilinear methods for dealing with LFM signals
  - Provides peaks for each LFM components in the FCR domain
  - Main merits:
    - High resolution/concentration
    - Asymptotic linear (very small cross-terms can be ignored)
    - Without increasing computational complexity

X. Lv, G. Bi, C. Wan, and M. Xing, Lv's distribution: principle, implementation, properties, and performance, IEEE TSP, vol. 59, no. 8, pp. 3576--3591, Aug. 2011.

# Lv distribution (LVD)

- **Definition** : a parametric symmetric instantaneous autocorrelation function (PSIAF) of the input signal  $x(t)$  :

$$R_x^C(t, \tau) = x\left(t + \frac{\tau + a}{2}\right)x^*\left(t - \frac{\tau + a}{2}\right) \rightarrow a : \text{constant time-delay}$$

auto-terms  $\rightarrow = \sum_{k=1}^K A_k^2 \exp(j2\pi f_k(\tau + a) + j2\pi \gamma_k(\tau + a)t)$

cross-terms  $\rightarrow + \sum_{i=1}^{K-1} \sum_{j=i+1}^K (R_{x_i x_j}^C(t, \tau) + R_{x_j x_i}^C(t + \tau))$

$t$  and  $\tau$  are coupled together, leading to cross term effects

- A scaling operator  $\Gamma$  of a phase function  $G$  with respect to  $(t, \tau)$  as

$$\Gamma[G(t, \tau)] \rightarrow G\left(\frac{t_n}{h(\tau + a)}, \tau\right)$$

$t_n = (\tau + a)ht$

$h$  : a scaling factor

# Lv distribution (LVD)

- Definition of the LVD

- Perform the scaling operation  $\Gamma$  on the PSIAF and obtain

$$\Gamma[R_x^C(t, \tau)] = \sum_{k=1}^K A_k^2 \exp\left(j2\pi[f_k(\tau+a) + \frac{\gamma_k}{h}t_n]\right) \rightarrow t \text{ and } \tau \text{ are decoupled}$$

$$+ \sum_{i=1}^{K-1} \sum_{j=i+1}^K \Gamma[R_{x_i x_j}^C(t, \tau) + R_{x_j x_i}^C(t, \tau)]$$

- Take the 2-D FT of the previous equation with respect to  $\tau$  and  $t_n$

$$L_x(f, \gamma) = F_\tau \left\{ F_{t_n} \left\{ \Gamma[R_x^C(t, \tau)] \right\} \right\} = \sum_{k=1}^K \underline{L_{x_k}(f, \gamma)} + \sum_{i=1}^{K-1} \sum_{j=i+1}^K \underline{L_{x_i x_j}(f, \gamma)},$$

auto-term                            cross-term

$$L_{x_k}(f, \gamma) = A_k^2 e^{j2\pi af} \delta(f - f_k) \delta\left(\gamma - \frac{\gamma_k}{h}\right)$$

# Lv distribution (LVD)

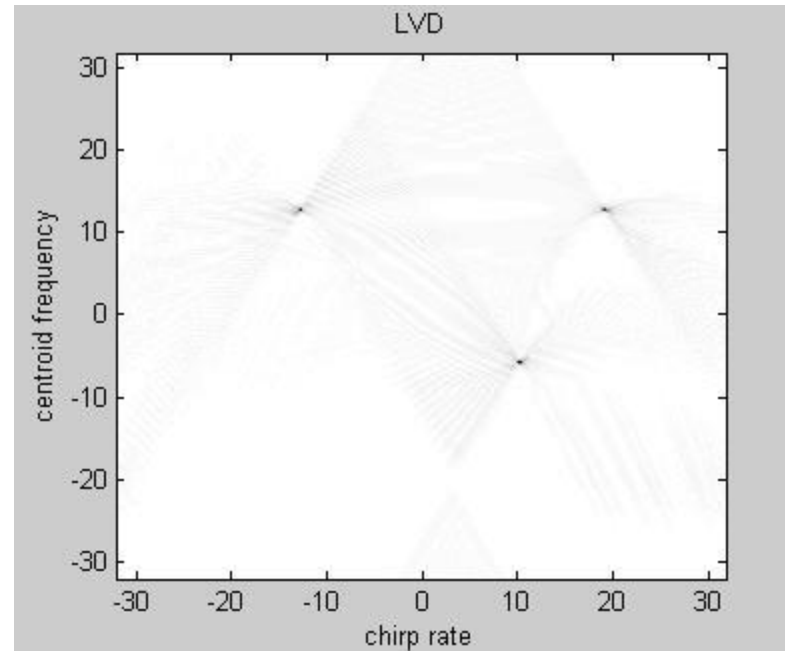
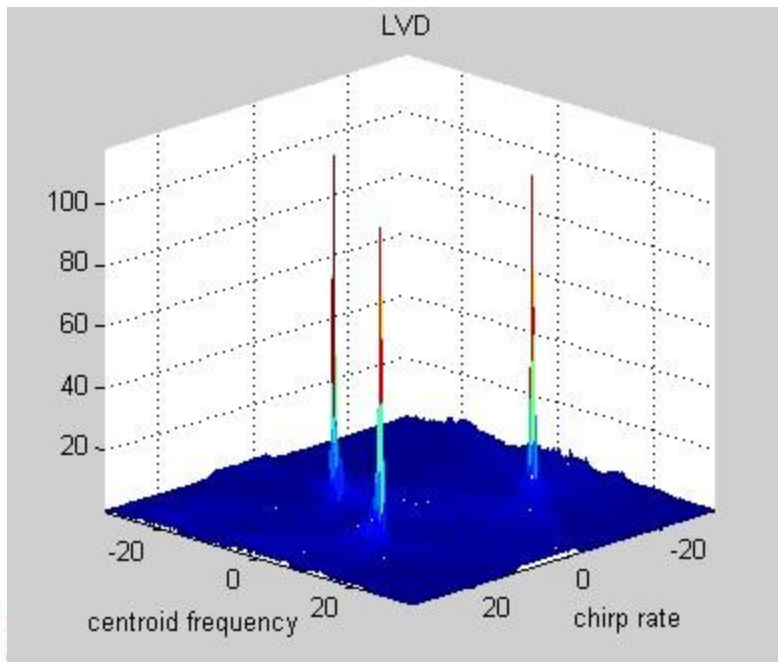
- Definition of the LVD

For a **multi-component LFM signal**, the LVD is **asymptotic linear** as

$$x(t) = \sum_{k=1}^K x_k(t) \rightarrow L_x(f, \gamma) \approx \sum_{k=1}^K L_{x_k}(f, \gamma).$$

The LVD has:

- three components;
- very little cross-terms;
- high resolution.



# Lv distribution (LVD)

- Properties of the LVD

- Asymptotic linear:

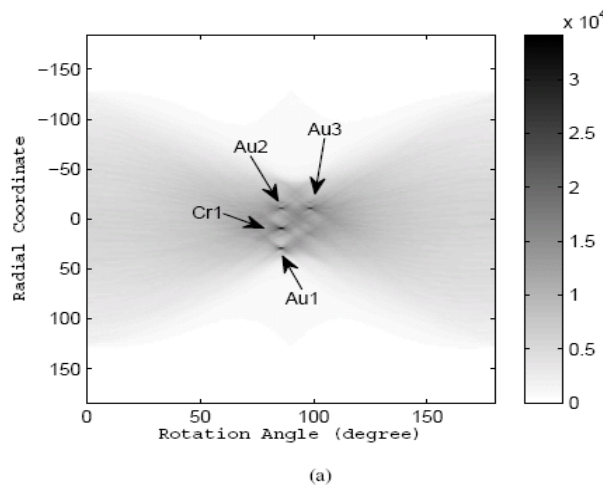
$$LVD[c_1x_1(t) + c_2x_2(t)] \approx |c_1|^2 LVD_{x_1}(f, \gamma) + |c_2|^2 LVD_{x_2}(f, \gamma)$$

- Frequency and chirp rate shift: if  $x_2(t) = x_1(t - t_0) \exp(j2\pi f_0 t) \exp(j\pi\gamma_0 t^2)$  we have  $LVD[x_2(t)] = e^{-j2\pi\gamma_0 t_0} e^{j2\pi f_0} LVD_{x_1}(f + \gamma_0 t_0 - f_0, \gamma - \gamma_0)$
  - Resolution:  $\Delta f = \frac{1}{T}$ ,  $\Delta\gamma = \frac{2}{T}$
  - Others: scaling, translation, convolution, etc.

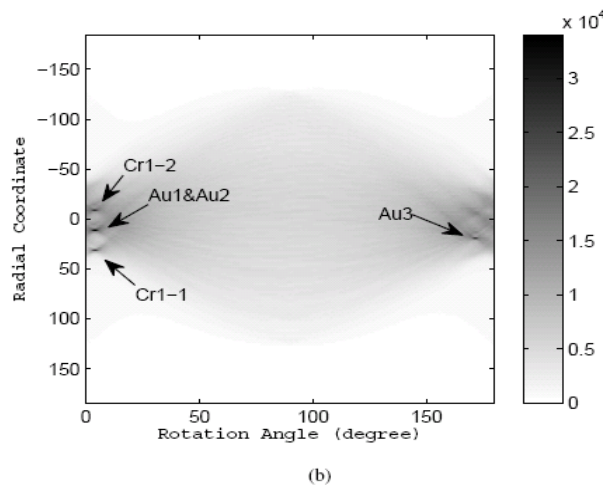
# Lv distribution (LVD)

- Performance of the LVD
  - Representation comparison

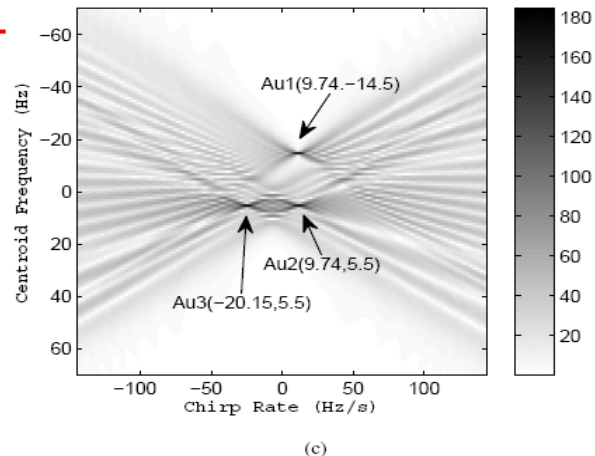
RWT



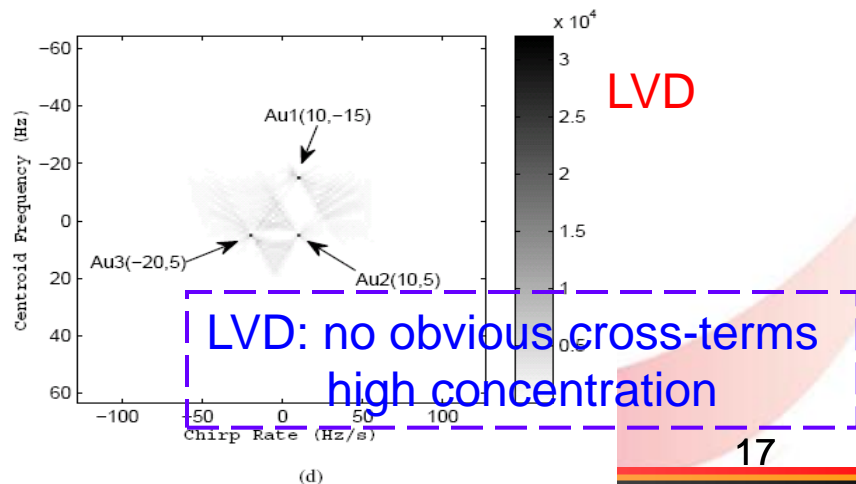
RAT



FrFT



LVD

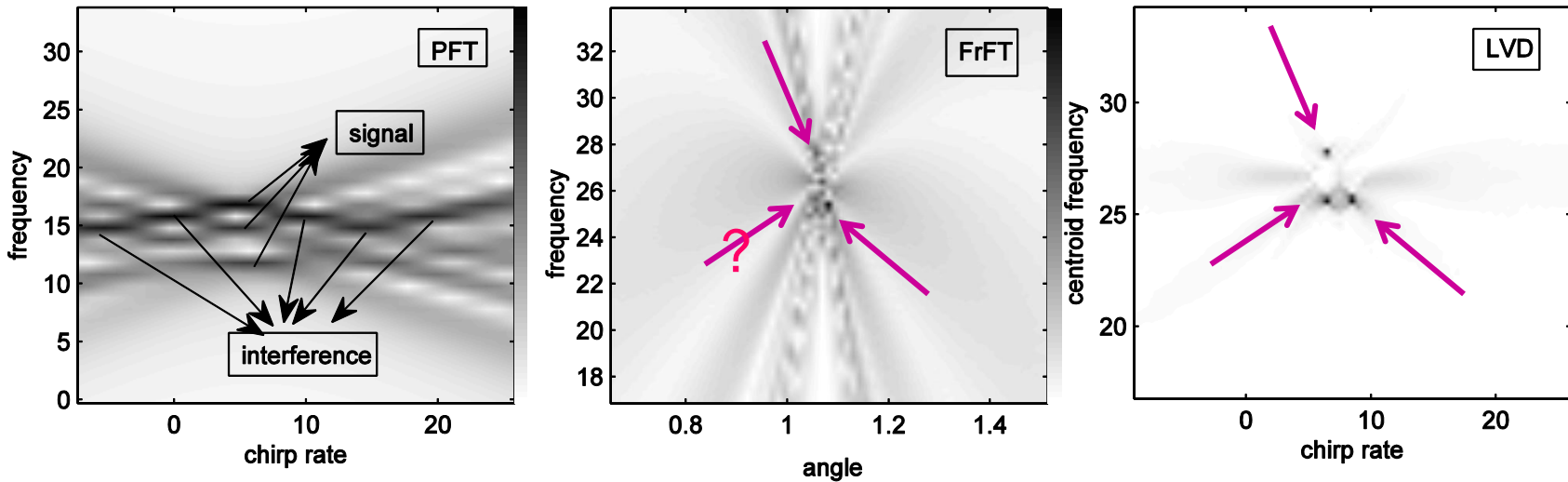


NANYANG  
TECHNOLOGICAL  
UNIVERSITY

# Lv distribution (LVD)

- Performance of the LVD
  - Resolution

Three LFM components with differences in centroid frequencies by 2 Hz and in chirp rates by 2 Hz/s ---- only the LVD can distinguish them

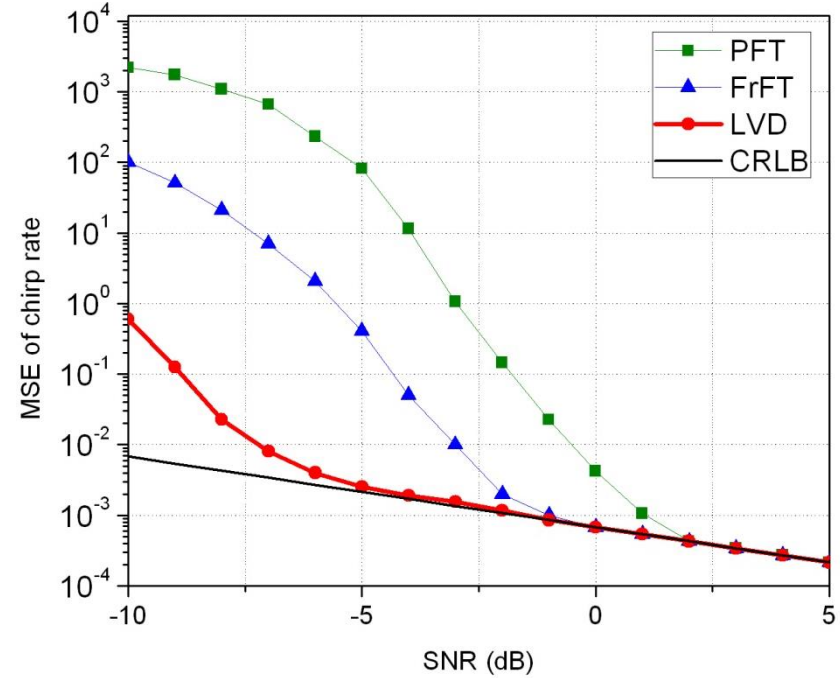
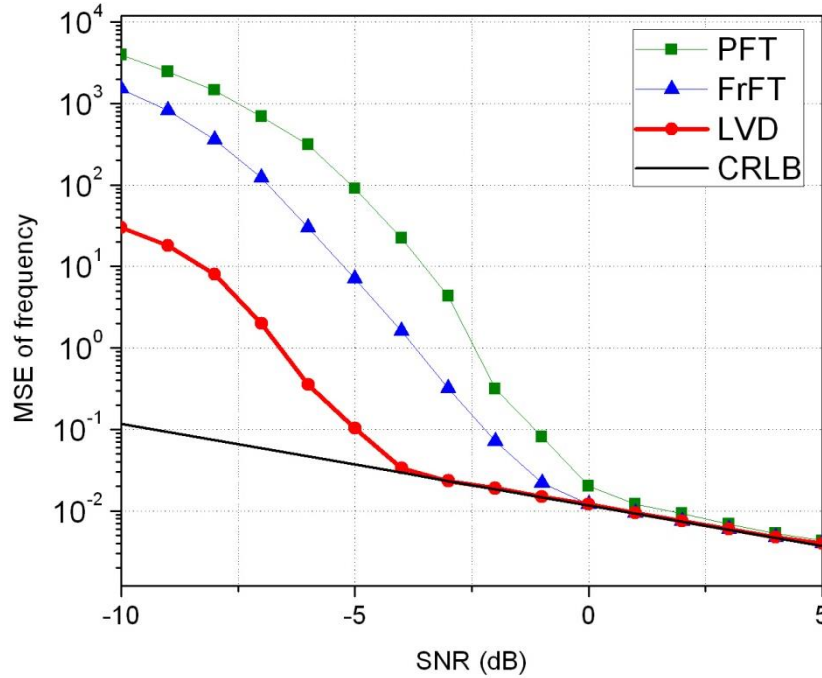


LVD: most narrow main-lobe width;  
highest resolution.

# Lv distribution (LVD)

- Performance of the LVD
  - Representation errors: mean square error (MSE)

$$MSE_{LVD,f} < \frac{147N^3 + 36f_s^2 N^2}{\pi^2 (98N^4 + 72f_s^4) SNR}, \quad MSE_{LVD,\gamma} < \frac{294}{\pi^2 N \cdot SNR}$$



MSEs of the LVD are lowest, and approach to the Cramer-Rao lower bounds (CRLBs) at lowest SNR

# Lv distribution (LVD)

- Performance of the LVD
  - Concentration: distribution concentration ratio (**DCR**)

$$DCR = 10 \log_{10} \frac{\text{ave} \left[ FCR(f, \gamma)_{(f, \gamma) \in S} \right]^2}{\text{ave} \left[ FCR(f, \gamma)_{(f, \gamma) \notin S} \right]^2}$$

higher DCR  
↓  
better concentration

- For mono-component LFM signal without noise, DCR of the LVD is

$$DCR_1 \approx 20 \log_{10} N \quad N: \text{data length}$$

- For K-component LFM signal without noise, DCR of the LVD is

$$DCR_K \approx DCR_1 - 20 \log_{10} K$$

DCR ↓ if signal component K ↑

# Lv distribution (LVD)

- Performance of the LVD

- Concentration:

- For noisy signal, DCR of LVD is

$$DCR_{K,SNR} = 10 \log_{10} \frac{1 + 2m_l / B_1 + (m_l^2 + \sigma_l^2) / B_1^2}{1 / D_K + 2Km_l / (N^2 B_1) + (m_l^2 + \sigma_l^2) / B_1^2}$$

$B_1 = A_1^2 T^2$ ,  $m_l = N \sigma_v^2$ ,  $\sigma_l^2 = N^2 \sigma_v^4 / 2$ ,  $\sigma_v^2$  is variance of input noise

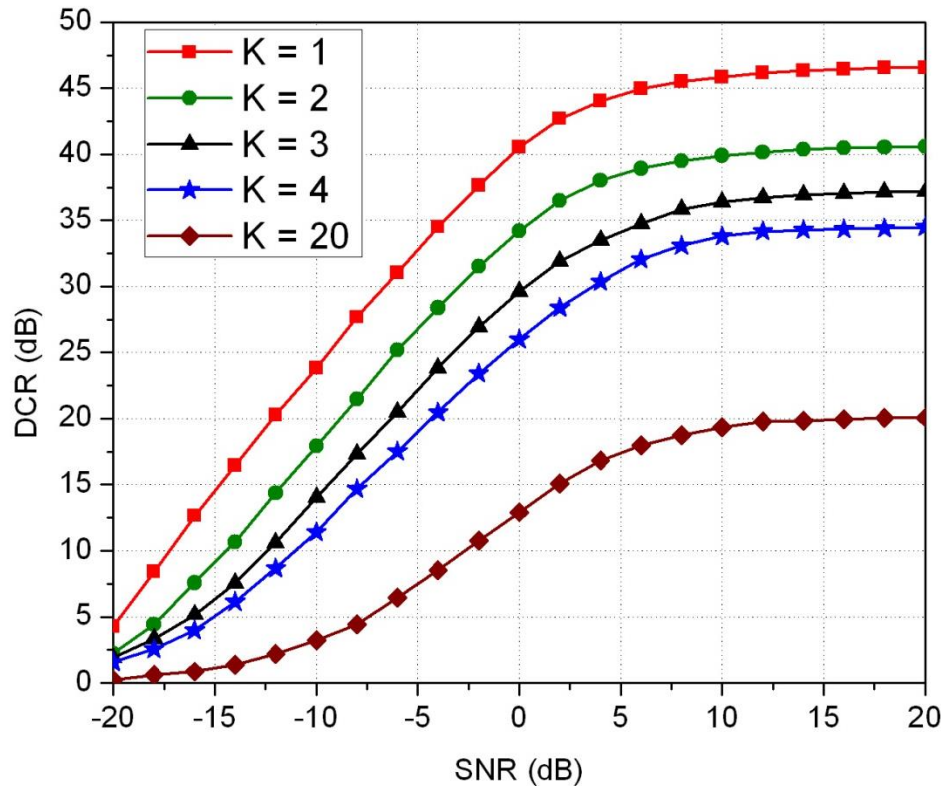
Easily to see,

$$\lim_{SNR \rightarrow +\infty} DCR_{K,SNR} = DCR_K$$

$$\lim_{SNR \rightarrow -\infty} DCR_{K,SNR} = 0$$

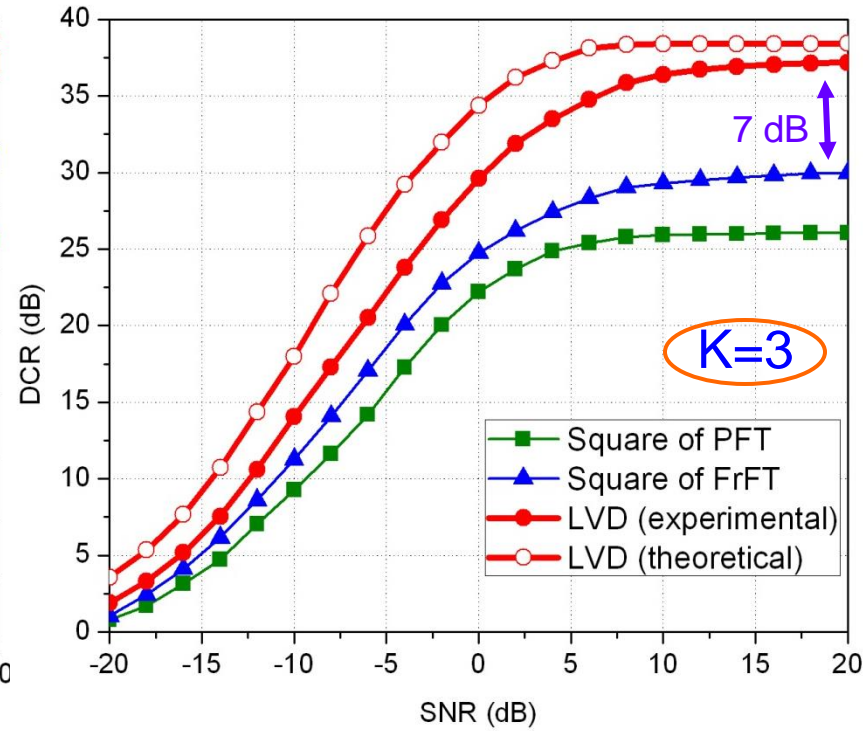
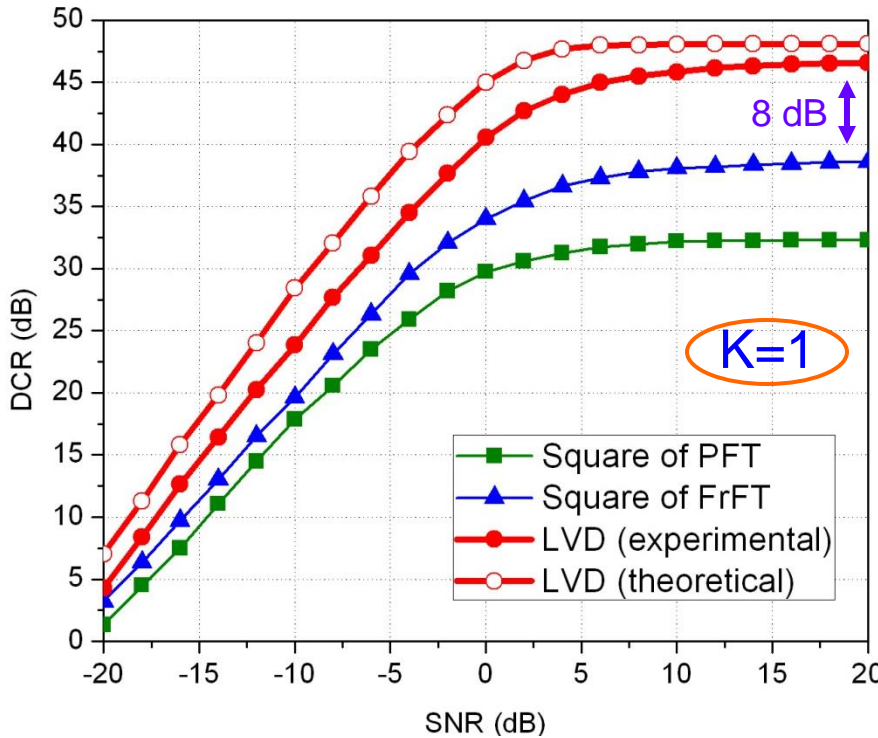
# Lv distribution (LVD)

- Performance of the LVD
  - Concentration:  
Experimental DCRs by using LVD in noisy environments



# Lv distribution (LVD)

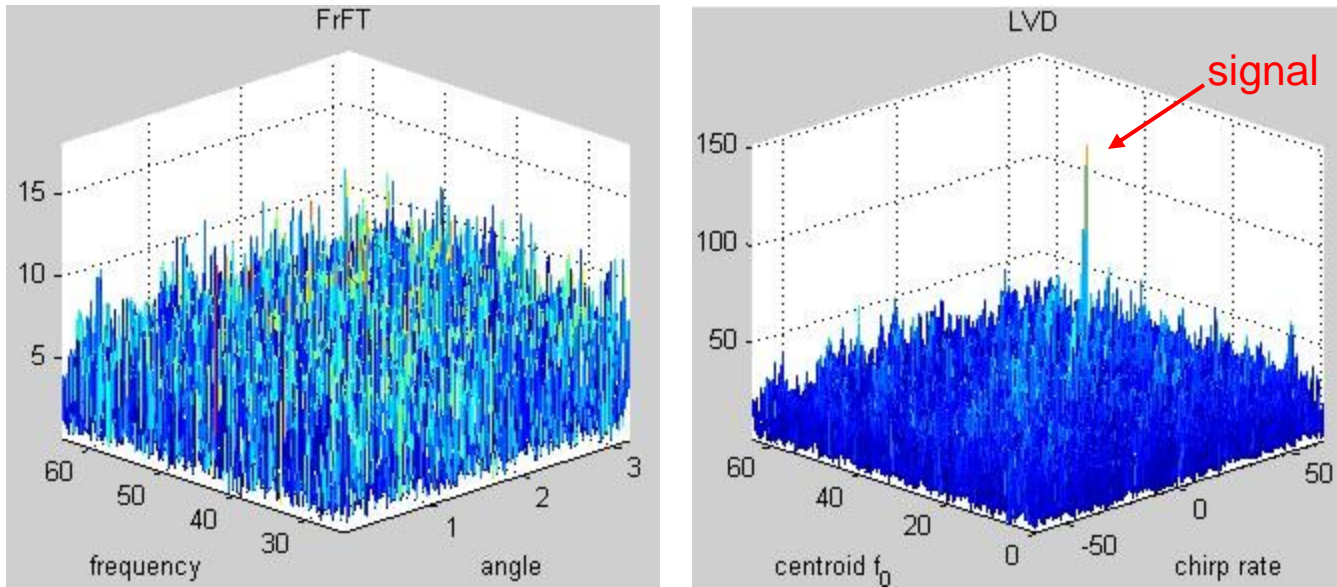
- Performance of the LVD
  - Concentration: Comparisons with PFT and FrFT



LVD concentrates better than  $|PFT|^2$  and  $|FrFT|^2$

# Lv distribution (LVD)

- Performance of the LVD
  - LFM signal Detection:  
Generally, better concentration leads to better detection.



FCRs under SNR = -13 dB

- The peak coordinates give the values of  $f_0$  and  $\gamma$

# Lv distribution (LVD)

- Performance of the LVD

- LFM signal Detection:

The **threshold** in LVD is

$$th_l = m_l + \sigma_l \Phi^{-1} (1 - P_{fa}) \quad P_{fa} : \text{false alarm probability}$$

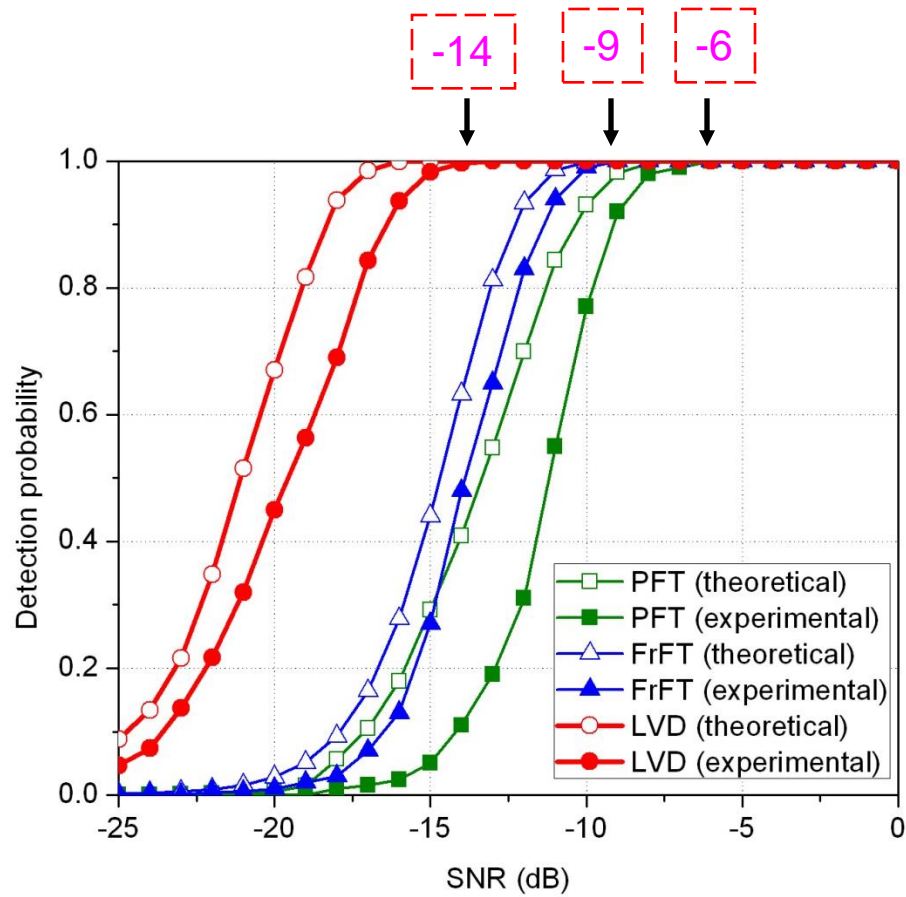
$\Phi(x)$  : cumulative distribution function  
of a standard normal distribution

and **theoretical detection probability** is

$$P_d = 1 - \Phi\left(\frac{th_l - m_{ls}}{\sigma_l}\right) \quad m_{ls} = m_l + L_s$$

# Lv distribution (LVD)

- Performance of the LVD
  - LFM signal Detection: Input sample length  $N = 512$



# Lv distribution (LVD)

- Performance of the LVD
  - Computational complexity

$$PFT: 2N_s^2 + N_s^2 \log_2 N_s \quad N_s : \text{input length}$$

$$FrFT: 4N_s^2 + N_s^2 \log_2 N_s$$

$$LVD: 2N_s + N_s^2 + N_s^2 \log_2 N_s$$

They are all in the **same** order of  $O(N_s^2 \log_2 N_s)$ , indicating that LVD provides better performance without introducing more computational complexity.

# Lv distribution (LVD)

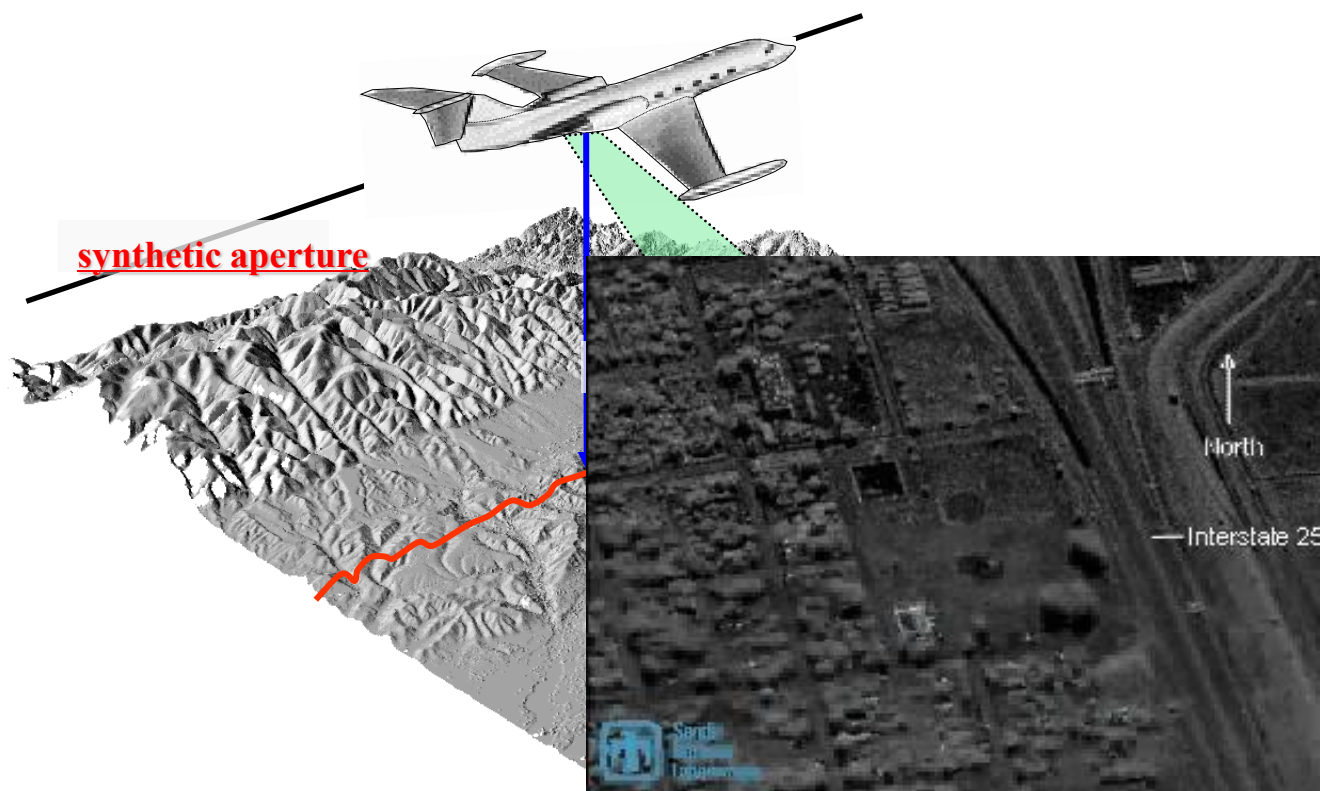
## ▪ Summary

- LVD directly obtains the centroid frequency and chirp-rate information
- LVD combines the merits of linear and bilinear properties for very low cross-term and high signal concentration, without requiring extra computation.
- Better resolution and signal detection performance than those from PFT and FrFT.
- **Shortcoming:** may not perform well for signal whose frequency changing very quickly because LVD requires relatively long delay related to the value  $a$ .

# Outline

- Introduction
- Lv distribution (LVD)
  - Definition, properties
  - Performances
- Application
  - SAR image processing
  - CS based SAR image processing
- Conclusion

# Synthetic Aperture Radar (SAR) Fundamental



L. Yang, G. Bi, M. Xing and L. Zhang, “Airborne SAR moving target signatures and imagery based on LVD,” IEEE Transactions on Geoscience and Remote Sensing, 2015, DOI: [10.1109/TGRS.2015.2429678](https://doi.org/10.1109/TGRS.2015.2429678).

# SAR Superiority



Optics Image



SAR Image

All Day/Night

All Weather

High Resolution

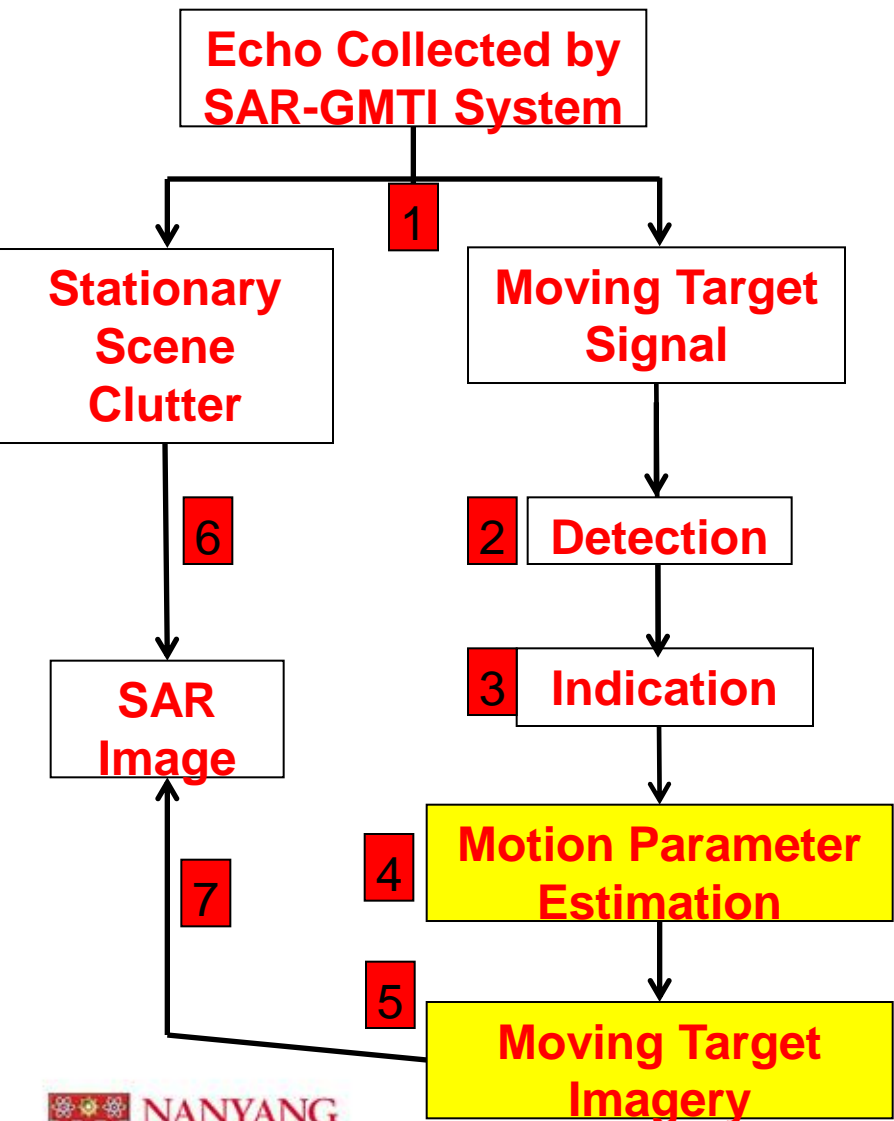
Independent

Long Range

Applications

Military: Monitor Warning; Target Surveillance;  
Defense Reconnaissance; Target Recognition; ...  
Civilian: Disaster Warning; Wounded Rescue;  
Vegetation Monitoring; Traffic Management; ...

# SAR Ground Moving Target Indication (GMTI)



- 1 SAR-GMTI System with Single-Channel or Multi-Channel; Separation of Clutter and Moving Targets; Clutter Suppression Using DPCA or STAP;
- 2 Moving Target Detection (CFAR);
- 3 Moving Target Indication (Classification);
- 4 Cross-track Velocity Estimation with Interferometry Phase; Along-track Velocity Estimation with Time-Frequency Distribution;
- 5 Target Relocation and Refocusing;
- 6 SAR Image Formation Algorithm;
- 7 Moving Target Marking on the SAR Image;

## Time-Frequency Based Moving Target Imaging

After clutter suppression, the phase history of each range cell containing one or multiple moving targets in range-compressed and azimuth slow-time domain can be modeled as:

$$s(t) = \sum_{i=0}^{I-1} A_i \exp(j2\pi f_i t + j\pi \gamma_i t^2)$$

$A_i$  is the amplitude

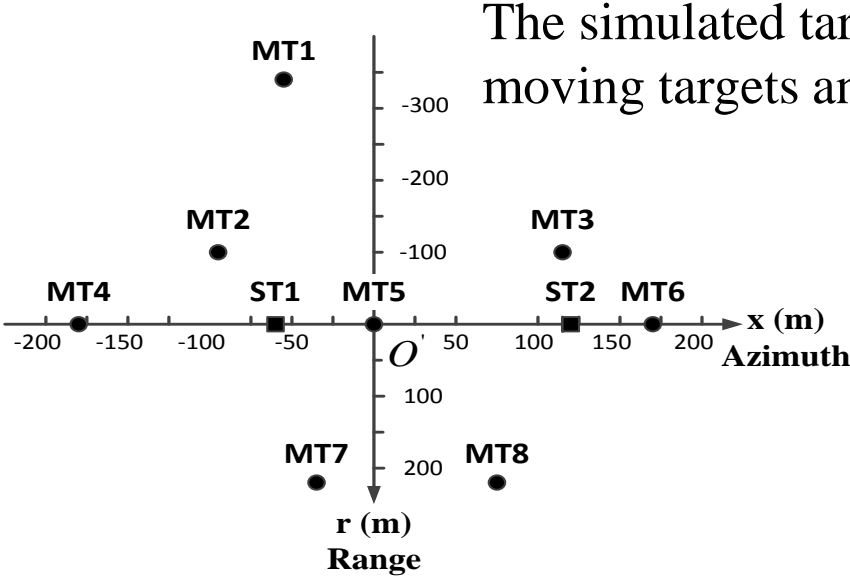
$f_i$  is the Doppler centroid frequency

$I$  is the target number

$\gamma_i$  is the Doppler chirp rate

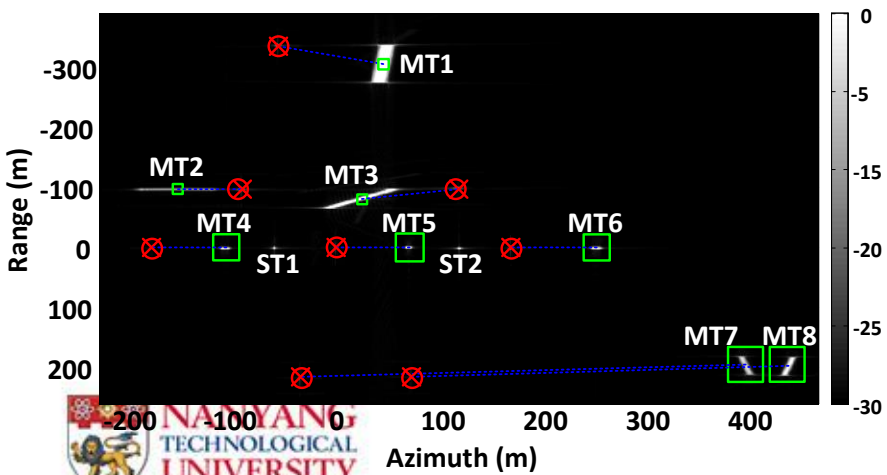
- Due to the target velocity in along- and cross-track will have Doppler frequency shift and Doppler frequency modulation in quadratic, respectively, the moving target image will be shifted and unfocused if no properly handled.
- The moving target phase history has the linear frequency modulation (LFM) form. Time-frequency analysis is more suitable.
- Based on the relationship between the centroid frequency and chirp rate and the velocity in along- and cross-track, the motion parameters can be expressed by time-frequency distribution (TFD).

# Simulations

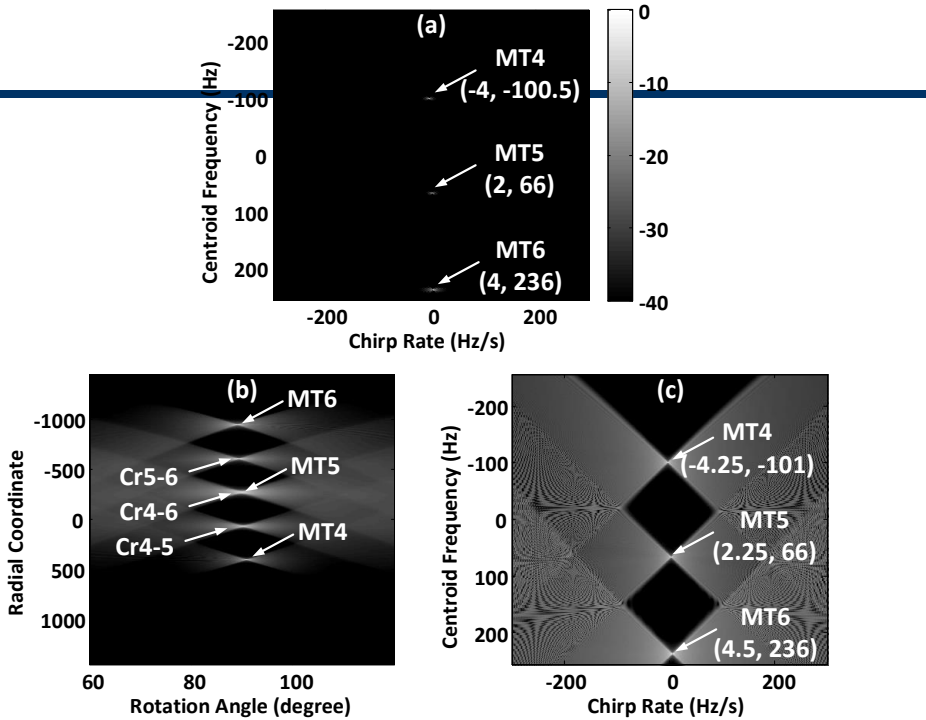


The simulated target ground truth for 8 moving targets and 2 stationary targets.

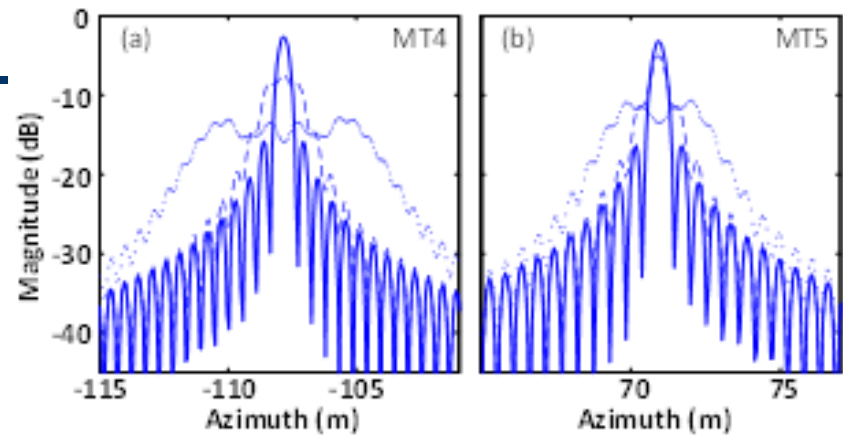
Simulated and estimated target velocities.					
	$v_x$ (m/s)	$v_r$ (m/s)	$\hat{v}_x$ (m/s)	$\hat{v}_r$ (m/s)	$m$
MT1	-2.0	30.0	-1.93	30.91	2
MT2	21.0	1.3	21.21	1.20	0
MT3	-15.0	17.0	-15.28	17.02	1
MT4	-2.1	-1.1	-2.08	-1.06	0
MT5	1.1	-1.0	1.11	-0.99	0
MT6	2.2	-1.2	2.25	-1.16	0
MT7	-2.2	-22.0	-2.24	-21.60	-1
MT8	2.1	-21.0	2.19	-20.59	-1



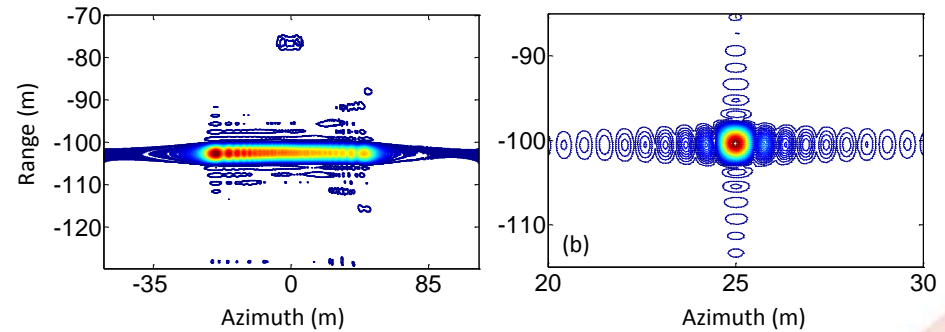
SAR moving target imaging results. Circle: moving target ground truth; Square: displaced and defocused moving target; Cross: geolocated and refocused moving target by the proposed algorithm.



TFR for MT4-MT6: (a) LVD, (b) RWT and (c) FrFT, (RWT is with rotational angle searching step  $0.1^\circ$ , and FrFT is with rotational order searching step 0.0002)



Azimuth responses of defocused and refocused (a) MT4, (b) MT5 (dotted line: defocused target response; dashed line: refocused target response based on FrFT representation; solid line: refocused target response based on LVD representation).



MT3 contour image ((a): range focused image after range walk correction; (b): final focused image).

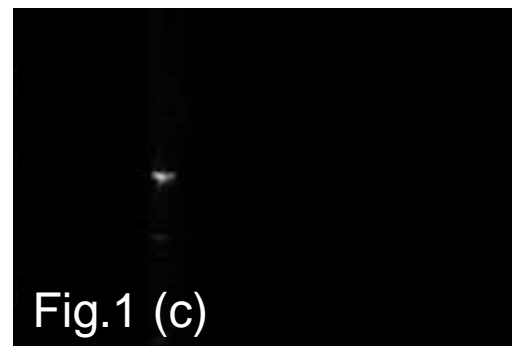
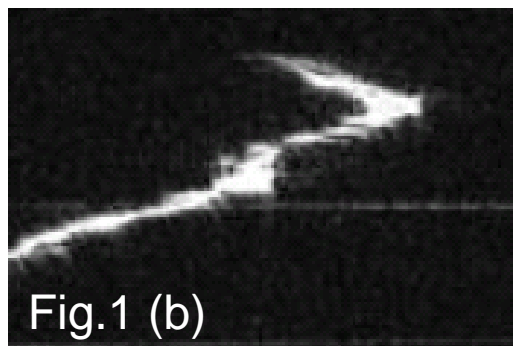
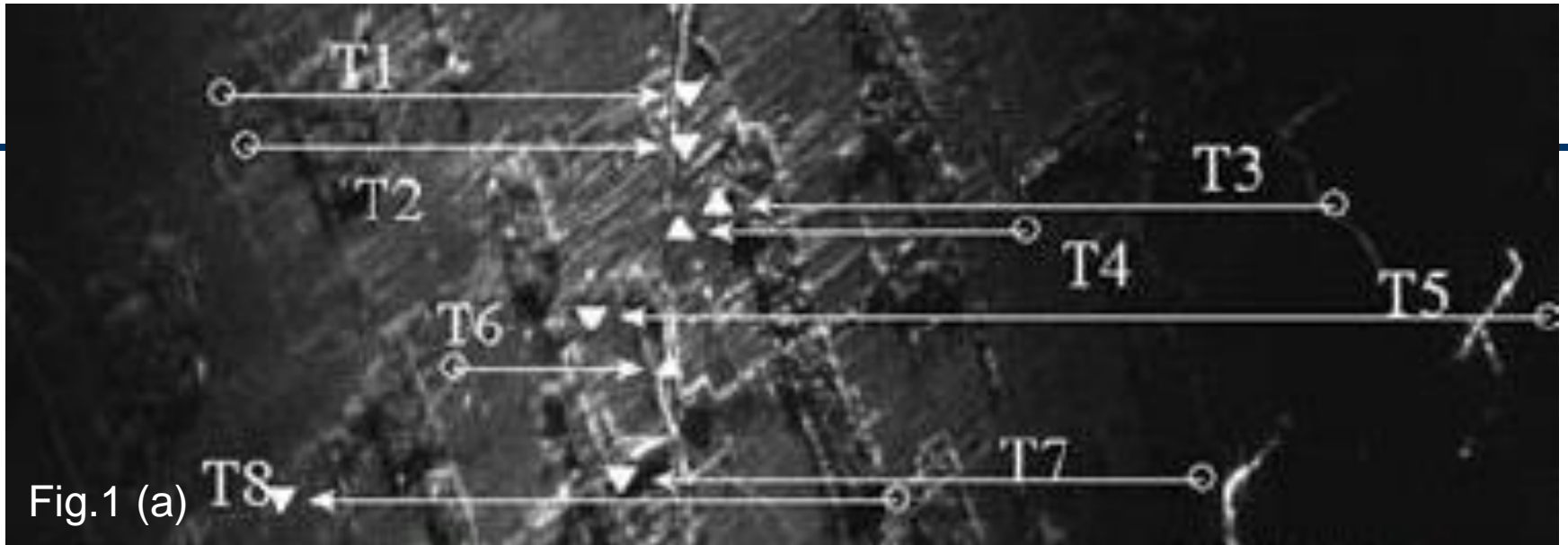


Fig. 1(a) is the SAR image with the moving targets by the raw SAR data; Fig. 1(b) is the defocused moving targets image of T6; Fig. 1(c) is the refocused moving targets image of T6;

# Outline

---

- Introduction
- Lv distribution (LVD)
  - Definition, properties
  - Performances
- Application
  - SAR image processing
  - **CS based SAR image processing**
- Conclusion

# Review on SAR Moving Target Imaging

## 1. Time-Frequency Representation

RWT (Radon Wigner transform): Bilinear --- Cross-terms [1].

FrFT (fractional Fourier transform): Linear but small dynamic amplitude range [2].

Based on the TFR, moving target image can be obtained simply by matched-filtering

## 2. Sparse Representation

Sparse Representation based method by constructing a large-scale over-complete dictionary [3].

- [1]. Guangcai Sun, Mengdao Xing, Xiang-Gen Xia, Yirong Wu, and Zheng Bao, “Robust ground moving-target imaging using deramp keystone processing,” IEEE TGRS, vol. 51, no. 2, pp. 966–982, Feb, 2013.
- [2]. Shengqi Zhu, Guisheng Liao, Yi Qu, Zhengguang Zhou, and Xiangyang Liu, “Ground moving targets imaging algorithm for synthetic aperture radar,” IEEE TGRS, vol. 49, no. 1, pp. 462–477, Jan., 2011.
- [3]. I. Stojanovic and W.C. Karl, “Imaging of moving targets with multi-static sar using an overcomplete dictionary,” IEEE JSTSP, vol. 4, no. 1, pp. 164–176, Feb 2010

# Motivation

- Improved Parameter Estimation by Lv's Distribution
  - True representation: for the LFM signal attributes or centroid frequency and chirp rate;
  - Asymptotic linearity: considerably low amplitude of cross-terms;
  - Analytical accuracy/resolution
  - High efficiency: fast Fourier transform (FFT) and complex multiplication;
- Improved Moving Target Imaging by Sparse Representation
  - Utilize the desirable statistical property of probabilistic modeling to make full use of sparse representation.
  - Obtain refined dictionary during estimation.

L. Yang, L. Zhao, G. Bi, SAR ground moving target imaging algorithm based on parametric and dynamic sparse Bayesian learning," Submitted to IEEE Transactions on Geoscience and Remote Sensing, 2015, Minor revised.

# Mathematical Model

After RCM is compensated in a multichannel Radar system, the range compressed signal for the  $i$ th channel becomes

$$\hat{s}_{i-0}(k_x) = A \cdot \exp \left( -j \left( k_x x + k_0 \frac{(R_0 + r)v_r}{R_0} \tilde{t}_n \right. \right. \\ \left. \left. + k_0 \left( \frac{(v - v_x)^2 + v_r^2}{2R_0} + \frac{(R_0 + r)a_r}{2R_0} - \frac{v^2}{2R_0} \right) \tilde{t}_n^2 \right) \right) \exp(j\Delta\phi_t(\tilde{t}_n)) + n_{i-0}$$

$n_{i-0}$  is the clutter residue and noise in range-compressed data domain including various deviations from the assumption of constant Doppler effect and ideal flight path.

Considering the finite signal length effect, the LVD representation is degraded into a sinc form

$$\left| \mathcal{L}_s(\hat{f}_d, \hat{\gamma}_d) \right| = \sum_{k=1}^K \Delta T^2 |A_k|^2 \text{sinc}^2 \left( \Delta T \left( \hat{f}_d - f_d^k \right) \right) \text{sinc}^2 \left( \frac{\Delta T}{2} \left( \hat{\gamma}_d - \gamma_d^k \right) \right)$$

$f_d^k$  and  $\gamma_d^k$ , there are resolution or accuracy

# Mathematical Model

- Considering the finite signal length effect, the LVD representation is degraded into a sinc form

$$\left| \mathcal{L}_s(\hat{f}_d, \hat{\gamma}_d) \right| = \sum_{k=1}^K \Delta T^2 |A_k|^2 \text{sinc}^2\left(\Delta T \left(\hat{f}_d - f_d^k\right)\right) \text{sinc}^2\left(\frac{\Delta T}{2} \left(\hat{\gamma}_d - \gamma_d^k\right)\right)$$

- The resolution accuracies are  $\rho_{f_d} = 1/\Delta T$  and  $\rho_{\gamma_d} = 2/\Delta T$ , and  $\otimes T$  is the coherence processing interval .
- Small  $\Delta T$  means wide width of the lobe and large  $\Delta T$  means deviation from the assumption of LFM.

# Mathematical Model

For simplification, we have the signal expression

$$s_t(t_n) = \exp(j\phi(t_n)) \sum_{i=1}^I \exp(j2\pi f_d(i)t_n + j2\pi\gamma_d(i)t_n^2) + c_n(t_n)$$

↓

$$\mathbf{Y} = \mathbf{EAX} + \mathbf{C}_n$$

**Y** represents the range-compressed and clutter-suppressed target signal measurements;

**E** gives the multiplicative perturbation as diagonal matrix

**A** is the dictionary with the form of quadratic modulated Fourier dictionary, where the quadratic parameter or chirp rate is determined according to the LVD representation;

**X** is the solution giving the focused SAR moving target image;

**C<sub>n</sub>** denotes the matrix for the unsuppressed clutter and noise

# Main challenge

1. The diagonal matrix  $\mathbf{E}$  is to be estimated,
2. The dictionary  $\mathbf{A}$  should be refined for more accuracy representation

Estimated Chirp rate from LVD

$$\downarrow$$
$$\mathbf{A} = \mathbf{A}(\gamma_d) = [\mathbf{A}_1, \dots, \mathbf{A}_K]$$

3. The sparse moving targets  $\mathbf{X}$  is to be estimated.

# Probabilistic Modeling

Commonly, the observation measurements are formulated as a Gaussian distribution

$$p(\mathbf{Y} | \mathbf{X}, \boldsymbol{\beta}) = \prod_{m=1}^M \mathcal{CN}\left(\mathbf{Y}_{:m} | \mathbf{EAX}_{:m}, \boldsymbol{\beta}_m^{-1} \mathbf{I}\right)$$

$$p(\mathbf{X} | \boldsymbol{\alpha}) = \prod_{m=1}^M \mathcal{CN}\left(\mathbf{X}_{:m} | 0, \boldsymbol{\Lambda}_m\right)$$

$$p(\boldsymbol{\alpha}_{:m} | \lambda_m) = \prod_{n=1}^N \Gamma(\alpha_{nm} | \eta, \lambda_m)$$

$$p(\lambda | a, b) = \prod_{m=1}^M \Gamma(\lambda_m | a, b)$$

$$p(\boldsymbol{\beta} | c, d) = \prod_{m=1}^M \Gamma(\beta_m | c, d)$$

$\beta$ : the inverse variance of the additive perturbation in each range cell  
Gamma distribution is imposed for convenient inference.

This hierarchical modeling makes the marginal distribution of  $x$  corresponding to a complex Laplace distribution to achieve sparsity.

# LVD based Sparse Bayesian Method for SAR GMTIm

**Step 1.** LVD representation to obtain  $\gamma_d$ , where the dictionary is constructed as  $A(\gamma_d)$  accordingly.

**Step 2.** While ~ Converge

**2a. Variational Expectation step to estimate the variables**

$$\Theta = \{X, \alpha, \lambda, \beta\}$$

**2b. Maximization step to estimate the parameter**

$$E, A$$

Output X.

- Dictionary A is constructed as a parametric one, with Doppler chirp rate initialized from LVD representation.
- Due to the discrete grid effects, the influence of the chirp rate mismatch in the dictionary cannot be simply neglected.
- Otherwise, the obtained SAR moving target image will not be fully focused. The proposed method can desirably cope with this problem by adaptively refining the dictionary during estimation.

---

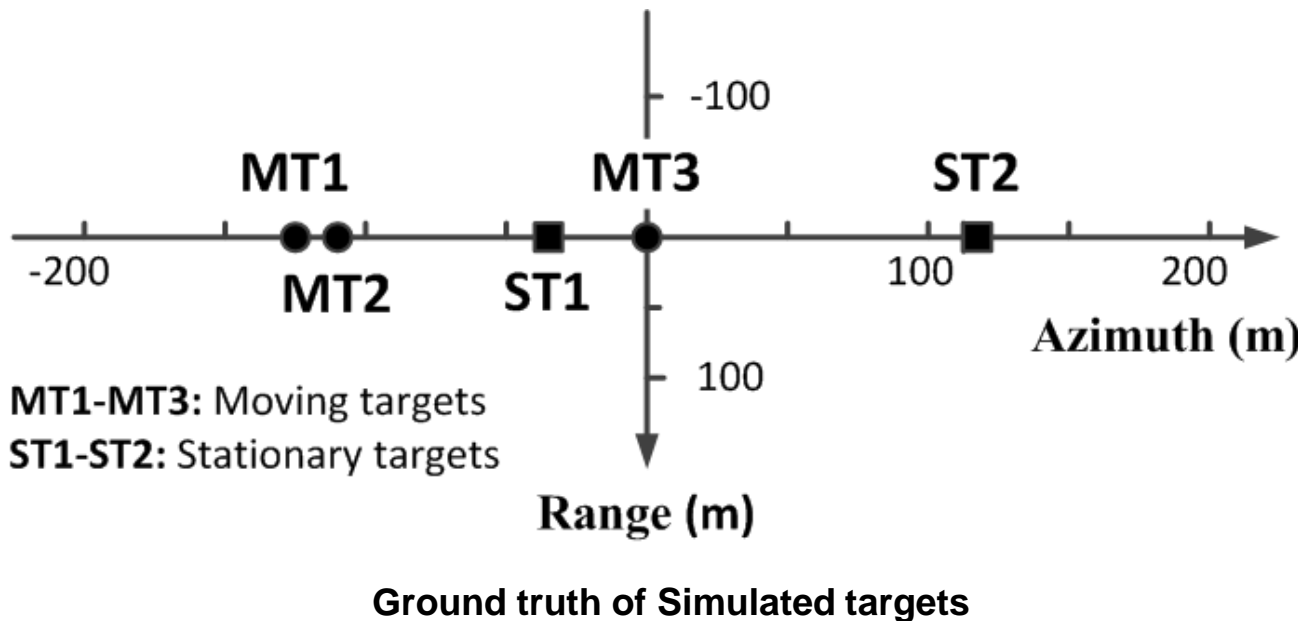
**Algorithm 1 : Parametric and Dynamic SBL for SAR-GMTIm**

---

1: **Input:** Range-compressed data after SAR image formation and multichannel clutter  
2:        suppression;  
3: **LVD:** Multiple moving target representation,  $\gamma_d$ ;  
4: **Initialization:**  $\mathbf{A}(\gamma_d)$ ,  $\mathbf{E}$ ,  $\alpha$ ,  $\lambda$ ,  $\beta$ ,  $a$ ,  $b$ ,  $c$ ,  $d$ ;  
5: **while** ~ Converge **do**  
6:     **I. Variational E-step**  
7:     **for**  $m = 1 : M$  **do**  
8:        Update  $\mu_{:m}$  and  $\Sigma_m$  by (43);  
9:        Update  $\alpha_{:m}$  by (45);  
10:      Update  $\lambda_m$  by (47);  
11:      Update  $\beta_m$  by (49);  
12:     **end for**  
13:     **II. Variational M-step**  
14:     **for**  $n = 1 : N$  **do**  
15:        Update  $\hat{\mathbf{E}}_{nn}$  by (53);  
16:     **end for**  
17:     **for**  $k = 1 : K$  **do**  
18:        Update  $\hat{\mathbf{A}}_k$  by (55);  
19:     **end for**  
20:     Construct  $\hat{\mathbf{A}}$  by  $\hat{\mathbf{A}} = [\hat{\mathbf{A}}_1, \dots, \hat{\mathbf{A}}_K]$ ;  
21: **end while**  
22: **Output:**  $\mathbf{X}$ ,  $\hat{\mathbf{E}}$ , and  $\hat{\gamma}_d$  or  $\hat{\mathbf{A}}$ .

---

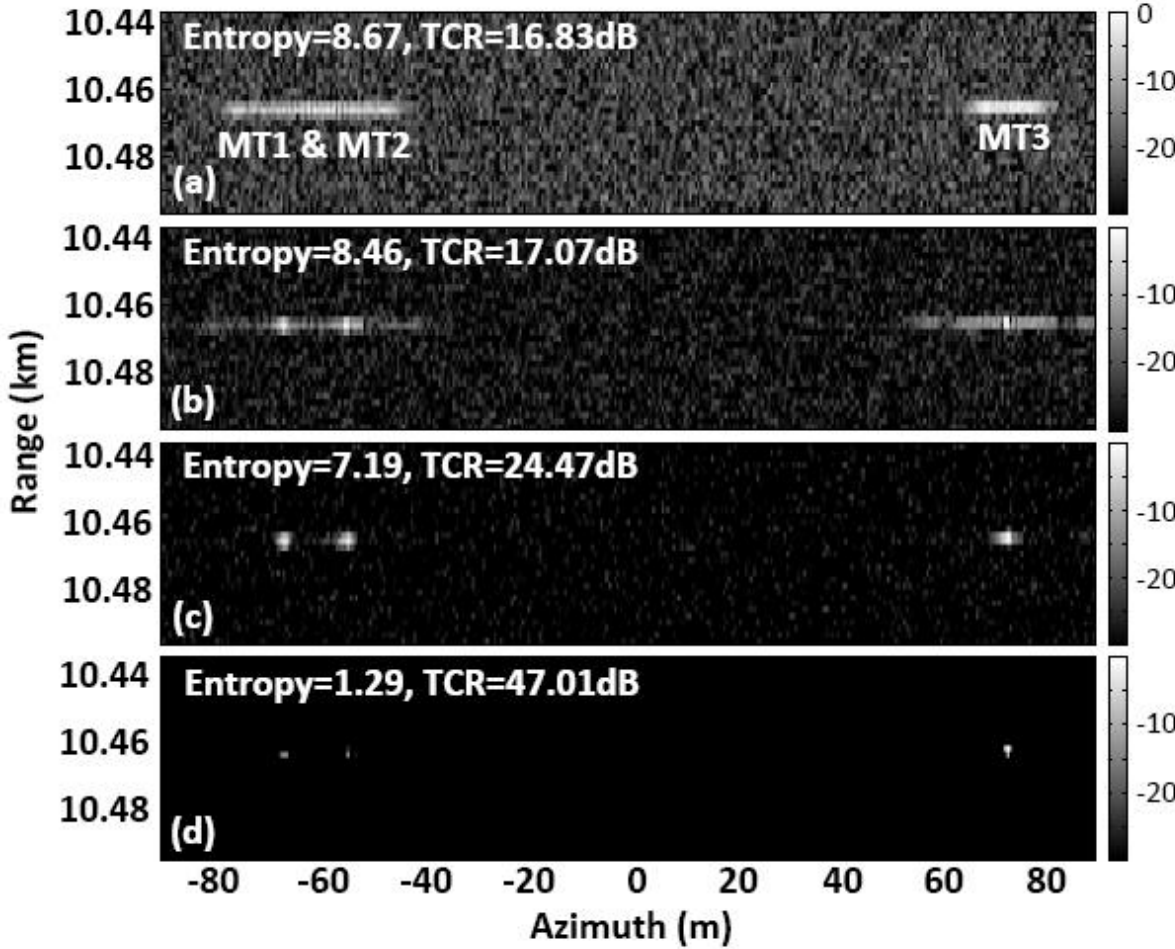
# Experiment Settings



- Target's velocities in slant- and cross-range obey a uniform distribution from 1 to 10m/s
- The accelerations in slant and cross-range obey a uniform distribution from 0 to 0.3m/s<sup>2</sup>.
- Amplitude of the residual clutter obeys Rayleigh distribution,
- Phase of the clutter obeys uniform distribution,
- Noise follows the Gaussian distribution with signal to clutter and noise ratio (SCNR)=3dB

# Experimental Results

Fourier  
Transform →

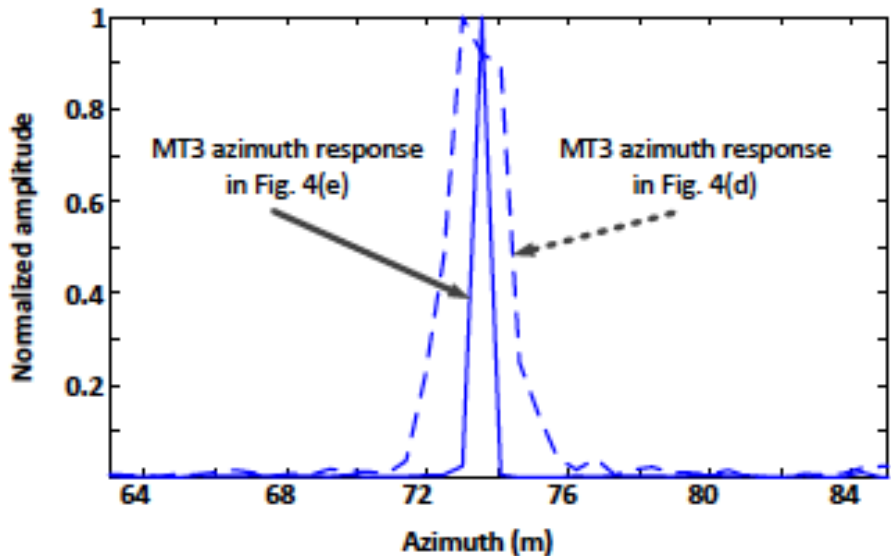


Matched  
Filter →

L1-Based  
Method →

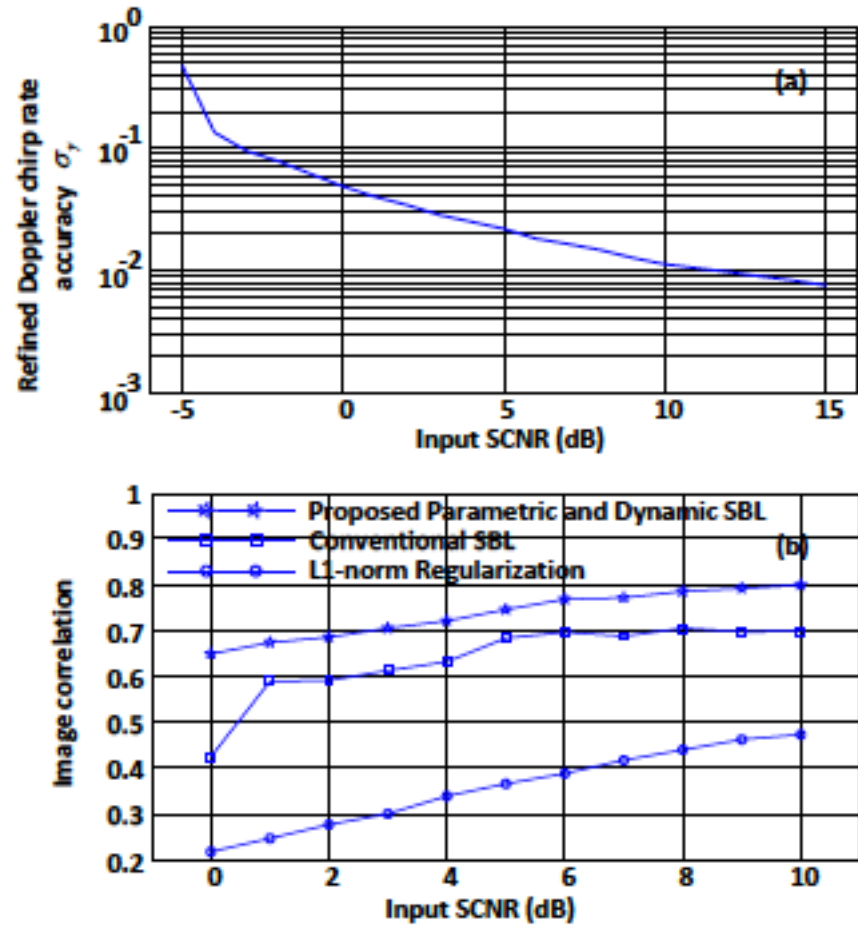
Proposed  
Method →

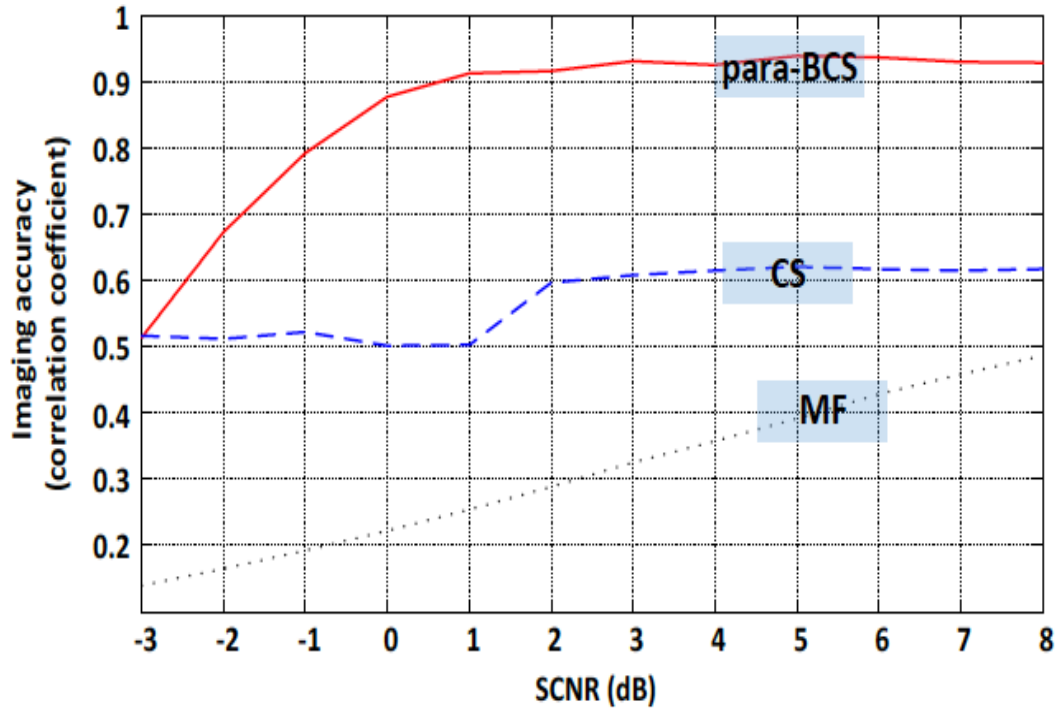
- Entropy: Measure the focusing quality;
- TCR (Target-to-clutter ratio): measure the image contrast;



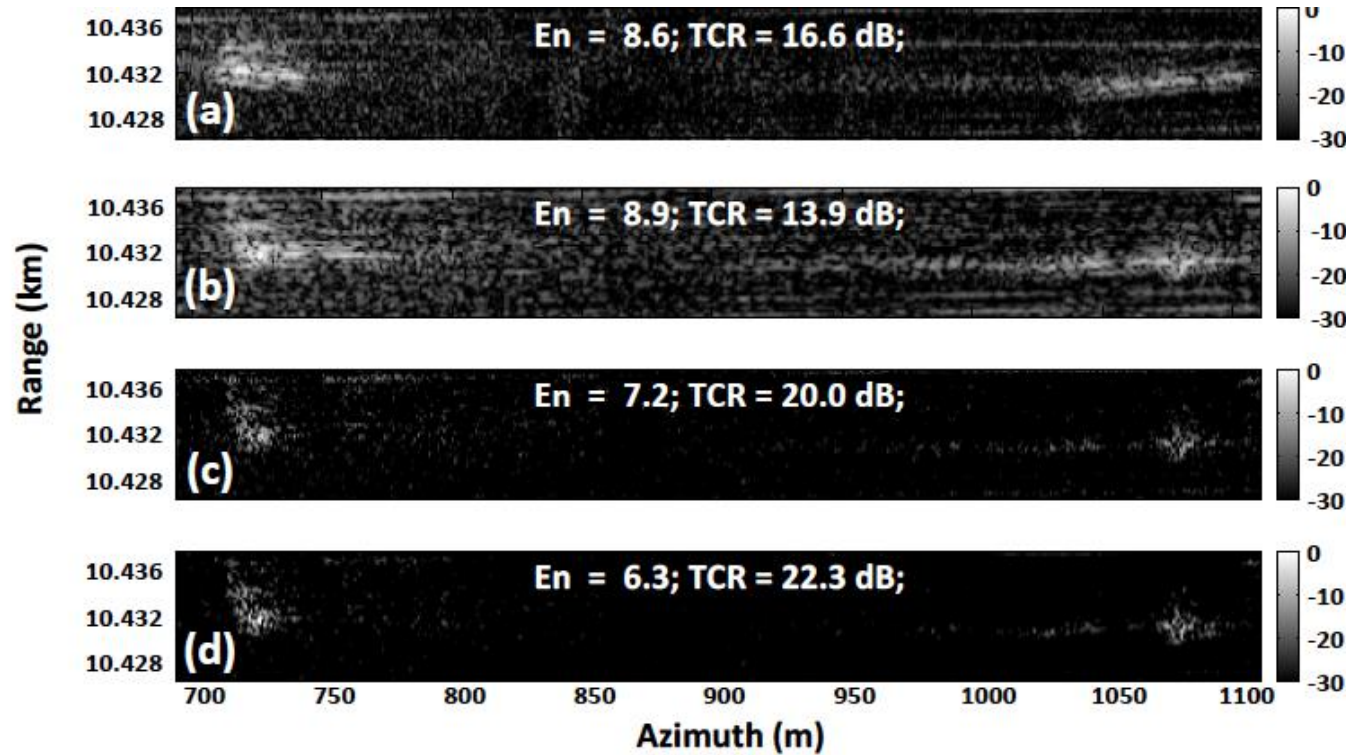
Azimuth responses of MT3 in Fig. 4(c) and (d)

Performance analysis in terms of SCNR. (a): Refined Doppler chirp rate accuracy; (b): Imaging accuracy.





Imaging accuracy comparison (1/2 under sampling data ratio and multiplicative phase error)



Real data processing results ((a): SAR image with 2 moving targets formed by FFT with full data sample; (b)-(d): SAR moving target image by MF, CS and para-BCS, respectively, 1/2 data undersampling ratio.

# Remarks

- LVD is to automatically represent **multiple** moving targets in the Doppler CFCR domain
- The proposed algorithm provides a dynamical refinement process for updating the LVD representative Doppler chirp rate integrated within the parametric SBL framework for better accuracy
- Both multiplicative phase error and additive clutter and noise are considered and formulated in the SBL framework to enhance moving target image

## Publications

1. [X. Lv, G. Bi, C. Wan, and M. Xing, Lv's distribution: principle, implementation, properties, and performance, IEEE TSP, vol. 59, no. 8, pp. 3576--3591, Aug. 2011.](#)
2. [L. Yang, G. Bi, M. Xing and L. Zhang, "Airborne SAR moving target signatures and imagery based on LVD," Accepted by IEEE Transactions on Geoscience and Remote Sensing, 2015.](#)
3. [L. Yang, L. Zhao, G. Bi, SAR ground moving target imaging algorithm based on parametric and dynamic sparse Bayesian learning," Submitted to IEEE Transactions on Geoscience and Remote Sensing, Minor revision, June. 2015.](#)
4. [L. Wang, L. Zhao, G. Bi, C. Wan and L. Yang, "Enhanced ISAR imaging by exploiting the continuity of the target scene," IEEE Trans. on Geosc. and Remote Sensing, vol. 52, no. 9, pp. 5736-5750, 2014.](#)
5. [L. Wang, L. Zhao, C. Wan and G. Bi, "Sparse representation based on ISAR imaging using Markov random fields," IEEE Journal of Selected Topics in Applied Earth Observations and Remote Sensing, DOI: 10.1109/JSTARS.2014.2359250.](#)
6. [L. Zhao, L. Wang, G. Bi, L. Yang and H. Zhang "Structured sparsity-driven autofocus algorithm for high-resolution radar imagery," Submitted to IEEE Jstar, 2015.](#)
  
1. [L. Wang, L. Zhao, G. Bi and H. Zhang, "Novel Wideband DOA Estimation based on Bayesian Compressive Sensing with Dirichlet Process Prior," Submitted to IEEE TSP, Minor revision, July 2015.](#)
2. [L. Zhao, L. Wang and G. Bi "Robust frequency-hopping spread spectrum estimation based on sparse Bayesian method," IEEE TWC, vol. 14, no. 2, pp. 791-793, Feb. 2015.](#)
  
3. [L. Wang, L. Zhao, G. Bi and C. Wan, "Hierarchical sparse signal processing recovery by variational Bayesian inference," IEEE SPL, vol. 21, no. 1, pp. 110-113, 2014.](#)
4. [L. Zhao, G. Bi, L. Wang and H. Zhang, "An improved auto-calibration algorithm based on sparse Bayesian learning framework," IEEE Signal Processing Letters, vol. 20, no. 9, pp. 889-892, 2013.](#)
5. [X. Lv, G. Bi and C. Wan, "The group lasso for stable recovery of block-sparse signal representations", IEEE Trans. on SP, vol. 59, no. 4, pp. 1371-1382, 2011.](#)

---

*Thank you!*